Supporting Information

Cotnoir-White et al. 10.1073/pnas.1716224115

SI Materials and Methods

Cell Lines and Reagents. HEK293T cells (Sigma-Aldrich) were grown in DMEM with 10% FBS (Wisent). Polyethyleneimine (PEI; 25-kDa molecular mass, linear or branched forms) was obtained from Sigma-Aldrich. Coelenterazine h and coelenterazine 400a were obtained from NanoLight Technology. 17-Beta-estradiol (E2) and 4-hydroxytamoxifen (OHT) were purchased from Sigma-Aldrich; RU58668 (RU58), ICI182,780 (ICI), and raloxifene (Ral) were purchased from Tocris Cookson. The Gibson assembly procedure was performed according to the manufacturer's protocol using Gibson Assembly Master Mix (New England BioLabs).

Expression Plasmids.

Donor plasmids: RLucII fusions. Full-length ERα and ERβ cDNAs were PCR-amplified from expression vectors for the human ESR1 and human ESR2 genes pSG5-HEG0 and pSG5-ERβ, respectively, and cloned in-frame N-terminal to RLucII into the NheI/BamHI restriction sites of pcDNA3.1(Hygro+)-RLucII vector DNA (1). V2R was cloned N-terminal to RLucII in the pcDNA3.1/Zeo(+) vector backbone (Thermo Fisher Scientific) between the NheI and BamH1 sites. βArr2-RlucII was cloned N-terminal to RLucII in the pcDNA3.1/Hygro(+) vector backbone between the NheI and HindIII sites.

Intermediate plasmids: mTFP1, mTagBFP2, and GFP2 fusions. CMV promoter-driven expression vectors for mTFP1 (monomeric form), mTagBFP2, or GFP2 were generated by replacement of the eGFP in the peGFP-N2 vectors (Clontech) with the cDNA for mTFP1 (Allele Biotechnology), mTagBFP2, or GFP2, which was inserted into the BamHI/NotI sites of peGFP-N2. Human full-length ERα and ERβ were cloned into the above-described vectors N-terminal to mTFP1, GFP2, or mTagBFP2 by PCR amplification of coding sequences and digestion of 5′ and 3′ ends with the appropriate restriction enzymes (EcoRI and BamH1) or by Gibson assembly. The ERα(L507R) mutant was created by site-directed mutagenesis. The Nur77-mTFP1 vector was a kind gift from D. Lévesque, Université de Montréal. The V2R cDNA was cloned by fusing it N-terminal to mTFP1 in pIRES-Puro3 (Clontech). The V2R-mTFP1 expression vector was generated by replacement of the Venus cDNA by mTFP1 between BamHI and Not1 of the pIRES-puro3-V2R-Venus expression vector (2).

Acceptor plasmids: YFP fusions. CMV promoter-driven expression vectors for Venus or Topaz (3–9) were generated by replacement of the eGFP in the peGFP-N1 vector (Clontech) with cDNAs for the corresponding fluorophores to generate pVenusN1 or pTopazN1, inserted between the AgeI and NotI sites. DsRed and mTagBFP2 (monomeric form) cDNAs were cloned into pcDNA3.1/Hygro(+). The CoA-Ven construct was generated by inserting tandem copies of oligonucleotides coding for the WT version of the first NCOA2 LXXLL motif (amino acids 641 to 645) or a mutated AXXAA version and for a glucocorticoid receptor-derived nuclear localization signal sequence (amino acids 467 to 503) into pVenus-N1 between the EcoRI and BamHI sites, and a second copy of Venus was added N-terminal to these motifs between the NheI and EcoRI sites to maximize energy transfer. ERα/β-interacting partners RID, AF1ID, PGC1α, LCoR, and SHP were similarly cloned between two copies of Topaz using PCR amplification and restriction enzyme digestion or Gibson assembly. The RID was cloned from SRC1/NCOA1 cDNA with primers flanking the third and fifth LXXLL motifs (amino acids 633 to 753). The AF1-interacting domain (AF1ID) encompasses the glutamine-rich region of SRC1/NCOA1 (amino acids 1,043 to 1,261). eYFP-SUMO3 and eYFP-SUMO1G expression vectors were obtained from M. Dasso, NIH, Bethesda, MD (10). Gγ2-Venus was cloned by insertion of Gγ2 C-terminal to Venus in pcDNA3.1/Hygro(+). βArr2 was subcloned from βArr2-meYFP (11) between the HindIII and BamHI sites of pVenus-N1 to generate βArr2-Venus.

Transfection Assays. HEK293T cells were maintained in DMEM supplemented with 10% FBS. Cells were switched to phenol red-free DMEM containing 10% charcoal-stripped FBS 2 d before transfection with ER expression plasmids. Cells were transfected using PEI (1.5 μg DNA, 1.5 μg PEI-branched, and 4.5 μg PEI-linear per 1.25×10^6 cells). DNA/PEI/cell suspensions were aliquoted in 96-well white-bottom culture plates (125,000 cells per well) for BRET, SRET, and BRETFect assays or in 12-well culture plates (1.25×10^6 cells per well) for spectral analysis and grown for 48 h before ligand treatment and signal quantitation.

BRET, BRETFect, and SRET Assays. The SRET spectral analysis (Fig. S2*C*) was performed similar to the corresponding BRETFect experiment with several changes to compensate for the dramatically decreased signal output (Fig. S1*E*). HEK293T cells were transfected with expression vectors for ERα-LucII, ERα-GFP2, and CoA-Venus (5 μg each per 1×10^7 cells). Cells were harvested 48 h posttransfection in HBSS 1× supplemented with 100 nM E2 and aliquoted in 96-well plates (2.5 million cells in 100 μL per well). Each well was scanned for 50 nm in 25-nm increments from 400 to 600 nm (400 to 450, 425 to 475, etc.). The seven resulting overlapping scans from different wells were fitted together to rebuild the spectrum of light emission from the SRET experiment.

Note that while an LP550 filter (TTO) was used in BRETFect to limit bleed-through from mTFP1 emission in BRETFect assays, use of a BP530-nm filter yielded similar delta BRET signals. The 485-nm CTOP filter combines detection of energy emitted by RLucII/coel-h and of the energy reemitted by mTFP1, and thus reflects the total energy available for transfer to the acceptor.

Net BRET values are BRET ratios for fused proteins minus BRET ratios with fused luciferase but unfused GFP. Delta BRETFect measurements were calculated by subtraction from the three-partner BRET ratios of the sum of those obtained in the D + A and D + I controls. Net SRET and delta SRET were calculated as for BRETFect but using previously described assay parameters (3). For titration analyses, BRET ratios were represented as a function of $\log_{10}$(fluorescent protein/CTOP), where levels of the fluorescent protein are measured after direct stimulation at the appropriate wavelength using a FlexStation II microplate reader. FRET ratios were calculated as (emission 550 nm)/(emission 495 nm). For individual spectral analysis, relative light units (RLUs) were calculated as the fraction of the maximal value recorded in each condition (arbitrarily set at 1.00). For comparison of the emission spectra under BRETFect and control conditions (Fig. 2 *A–D*), spectra were standardized for the total area under the curve (AUC) to reflect energy redistribution.

All graphs were generated using GraphPad Prism 5.00, which analyzed titration data using nonlinear regression curve fit with variable slope [log(agonist) vs. response] and one-way ANOVA and the Bonferroni post hoc test. Spectral analysis was performed by AUC quantification using GraphPad Prism 5.00.

BRETFect and FRET Time Course Experiments. For time course experiments, cells were transfected as indicated above and treated at time 0. Luminescence was then measured approximately every

30 s for BRET and 60 s for FRET. Data presented in Fig. 6 *B* and *D* are the subtraction (delta BRET) of the BRET signals obtained in nontreated cells from the AVP-treated signals. BRET and FRET ratio measurements in the presence or absence of AVP are presented in Fig. S6 *B*, *C*, *F*, and *G* as a function of time (relative BRET ratios with respect to values at time 0).

Western Analysis. For Western analysis, HEK293T cells were seeded into 10-cm dishes at a density of 2×10^6 cells per plate. The following day, cells were transfected (1 μg of ERα-expressing vector per plate) with PEI as described above and then treated 48 h later with ICI182,780 (1 μM) or vehicle (0) for 1 h. Cells were harvested in ice-cold PBS, and whole-cell extracts were prepared by lysis in extraction buffer [Tris·HCl, pH 7.4, 50 mM; EDTA, 5.0 mM; NaCl, 150 mM; Triton X-100, 0.5%; Nonidet P-40, 1.0%; SDS, 2%; freshly added protease inhibitors (PMSF 1%, leupeptin 0.1%, pepstatin 0.1%, aprotinin 0.1%); *N*-ethylmaleimide, 2 mM]. Extracts were homogenized by sonication and quantified by Lowry assay (Bio-Rad). Equal amounts of proteins (50 μg) were separated on an SDS/polyacrylamide gel (7% acrylamide) and transferred onto PVDF membranes (Millipore). Membranes were hybridized with the appropriate antibodies (rabbit monoclonal anti-ERα antibody clone 60C, EMD Millipore; mouse monoclonal anti-ERβ 14C8, GeneTex; monoclonal mouse anti–alpha-tubulin clone DM1A, Sigma-Aldrich; monoclonal mouse anti–beta-actin, Sigma-Aldrich; mouse monoclonal anti-GFP B-2 antibody, Santa Cruz Biotechnology). Immunodetection was performed using enhanced chemiluminescence (PerkinElmer Life and Analytical Sciences) as recommended by the manufacturer, and detected using a ChemiDoc imager (Bio-Rad).

1. Breton B, et al. (2010) Multiplexing of multicolor bioluminescence resonance energy transfer. *Biophys J* 99:4037–4046.
2. Hamdan FF, Audet M, Garneau P, Pelletier J, Bouvier M (2005) High-throughput screening of G protein-coupled receptor antagonists using a bioluminescence resonance energy transfer 1-based beta-arrestin2 recruitment assay. *J Biomol Screen* 10:463–475.
3. Carriba P, et al. (2008) Detection of heteromerization of more than two proteins by sequential BRET-FRET. *Nat Methods* 5:727–733.
4. Ai HW, Henderson JN, Remington SJ, Campbell RE (2006) Directed evolution of a monomeric, bright and photostable version of *Clavularia* cyan fluorescent protein: Structural characterization and applications in fluorescence imaging. *Biochem J* 400:531–540.
5. Cubitt AB, et al. (1995) Understanding, improving and using green fluorescent proteins. *Trends Biochem Sci* 20:448–455.
6. Subach OM, Cranfill PJ, Davidson MW, Verkhusha VV (2011) An enhanced monomeric blue fluorescent protein with the high chemical stability of the chromophore. *PLoS One* 6:e28674.
7. Patterson GH, Knobel SM, Sharif WD, Kain SR, Piston DW (1997) Use of the green fluorescent protein and its mutants in quantitative fluorescence microscopy. *Biophys J* 73:2782–2790.
8. Zimmermann T, Rietdorf J, Girod A, Georget V, Pepperkok R (2002) Spectral imaging and linear un-mixing enables improved FRET efficiency with a novel GFP2-YFP FRET pair. *FEBS Lett* 531:245–249.
9. Piston DW, Patterson GH, Lippincott-Schwartz J, Claxton NS, Davidson MW (2017) Introduction to fluorescent proteins. Available at https://www.microscopyu.com/techniques/fluorescence/introduction-to-fluorescent-proteins. Accessed February 4, 2018.
10. Percherancier Y, et al. (2009) Role of SUMO in RNF4-mediated promyelocytic leukemia protein (PML) degradation: Sumoylation of PML and phospho-switch control of its SUMO binding domain dissected in living cells. *J Biol Chem* 284: 16595–16608.
11. Violin JD, Ren XR, Lefkowitz RJ (2006) G-protein-coupled receptor kinase specificity for beta-arrestin recruitment to the beta2-adrenergic receptor revealed by fluorescence resonance energy transfer. *J Biol Chem* 281:20577–20588.

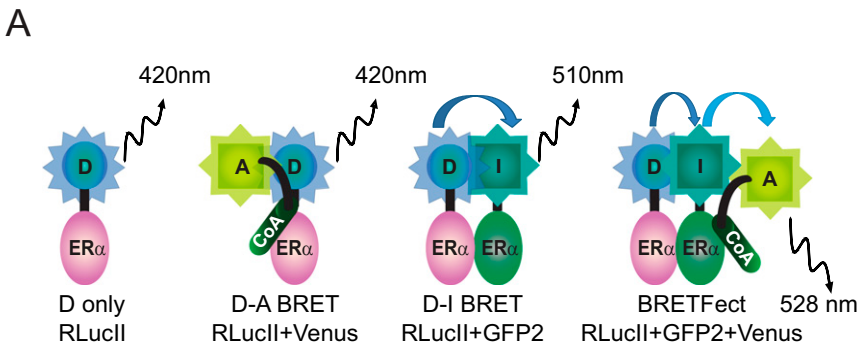

B

Role	Protein-tag	Exc (nm)	Em (nm)	Ext Coef	Quant Yield
D	RLucII / coel-400a		420		
	RLucII / coel-h		484		
I	mTFP1	462	492	64000	0.85
	GFP2	420	510	56500	0.55
	mTagBFP2	399	454	50600	0.64
A	Venus	515	528	92200	0.57
	Topaz	514	527	94500	0.60
	eYFP	514	527	83400	0.61
	DsRed	558	583	75000	0.79

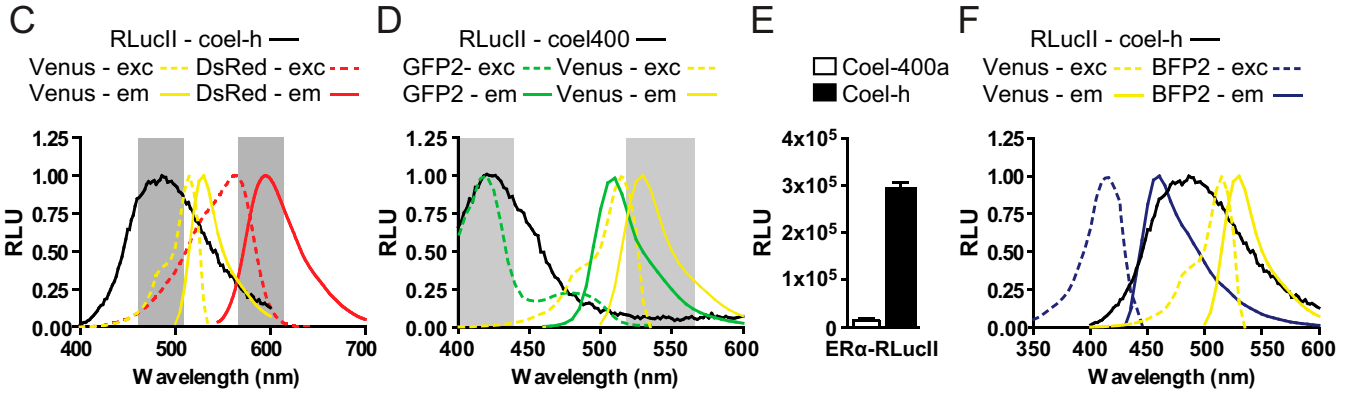

Fig. S1. (*A*) Description of donor ERα-RLucII (D), intermediate ERα-GFP2 (I), and acceptor CoA-Venus (A) fusion proteins and schematized energy transfer in the presence of two or three partners in a SRET[2] assay. (*B*) Physical constants of the different chromophores used in the SRET and BRETFect assays presented in this study (1–7). (*C*) Spectral profiles of the SRET[1] donor (RLucII/coel-h; black line), intermediate (Venus; yellow lines), and acceptor (DsRed; red lines). RLUs were calculated as the fraction of the maximal value recorded in each condition (arbitrarily set at 1.00). (*D*) Spectral profiles of the SRET[2] donor (RLucII/coel-400a; black line), intermediate (GFP2; green lines), and acceptor (Venus; yellow lines). (*E*) Comparison of luminescent signal output upon conversion of coel-h or coel-400a by RLucII. HEK293T cells were transfected with expression vectors encoding ERα-RLucII and unfused mTFP1 as a transfection control. Cells were treated with coel-h or coel-400a and luminescence was measured at 485 nm for coel-h and 400 nm for coel-400a. RLUs are luminescence counts normalized for transfection efficiency by fluorescence from unfused mTFP1. Error bars represent the SEM. (*F*) Spectral profile of mTagBFP2 (BFP2) as a "poor-transfer" intermediate control.

1. Carriba P, et al. (2008) Detection of heteromerization of more than two proteins by sequential BRET-FRET. *Nat Methods* 5:727–733.
2. Ai HW, Henderson JN, Remington SJ, Campbell RE (2006) Directed evolution of a monomeric, bright and photostable version of *Clavularia* cyan fluorescent protein: Structural characterization and applications in fluorescence imaging. *Biochem J* 400:531–540.
3. Cubitt AB, et al. (1995) Understanding, improving and using green fluorescent proteins. *Trends Biochem Sci* 20:448–455.
4. Subach OM, Cranfill PJ, Davidson MW, Verkhusha VV (2011) An enhanced monomeric blue fluorescent protein with the high chemical stability of the chromophore. *PLoS One* 6:e28674.
5. Patterson GH, Knobel SM, Sharif WD, Kain SR, Piston DW (1997) Use of the green fluorescent protein and its mutants in quantitative fluorescence microscopy. *Biophys J* 73:2782–2790.
6. Zimmermann T, Rietdorf J, Girod A, Georget V, Pepperkok R (2002) Spectral imaging and linear un-mixing enables improved FRET efficiency with a novel GFP2-YFP FRET pair. *FEBS Lett* 531:245–249.
7. Piston DW, Patterson GH, Lippincott-Schwartz J, Claxton NS, Davidson MW (2017) Introduction to fluorescent proteins. Available at https://www.microscopyu.com/techniques/-fluorescence/introduction-to-fluorescent-proteins. Accessed February 4, 2018.

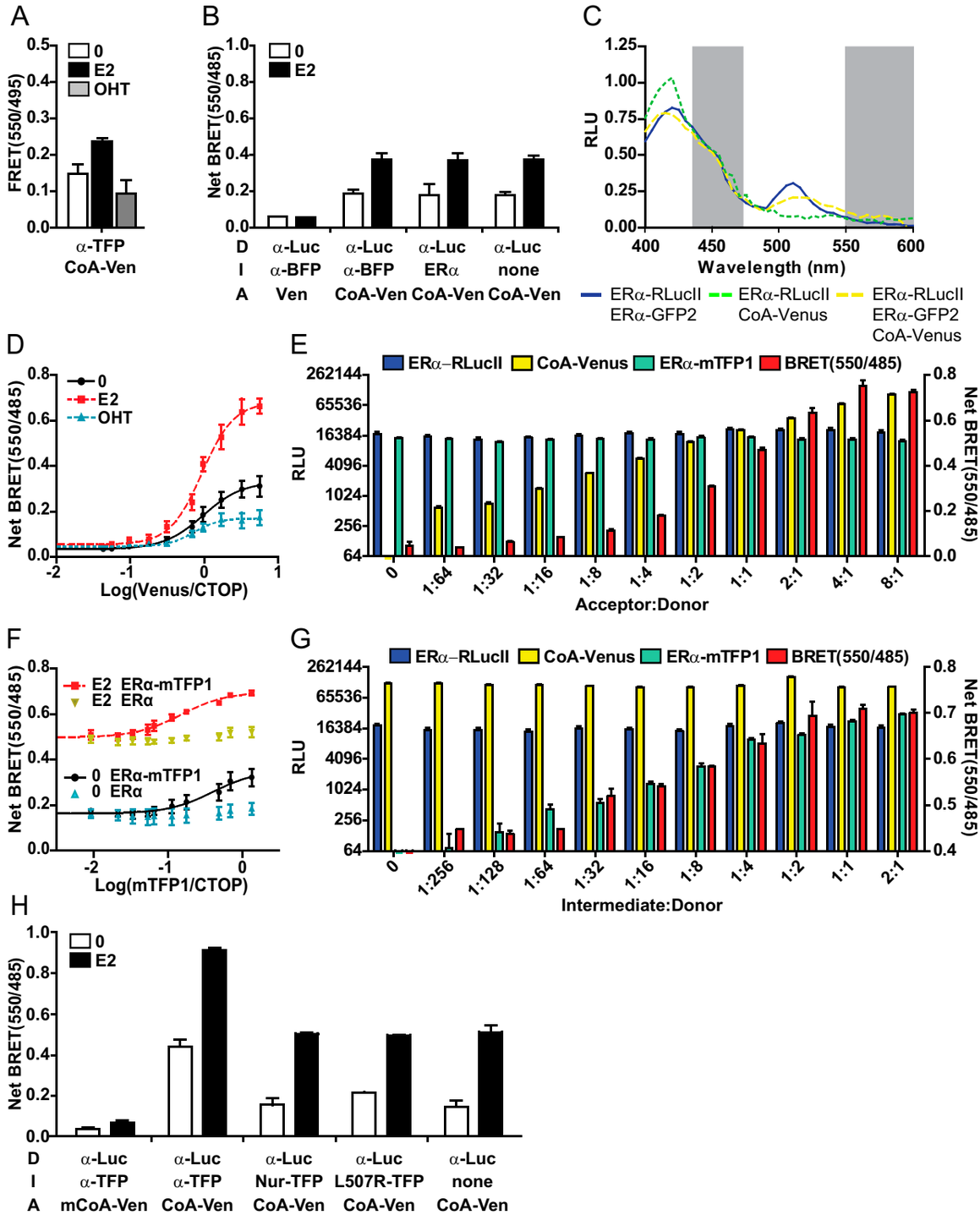

Fig. S2. (*A*) FRET between the intermediate and acceptor in the BRETFect assay from Fig. 2. FRET(550/495) ratios were measured from HEK293T cells transfected with ERα-mTFP1 and CoA-Venus and treated with ligands (E2 or OHT) or with vehicle only (0) for 45 min. Values reported are the average of three biological replicates ($n = 3$), each measured from three technical replicates. Error bars represent the SEM. (*B*) Control condition using mTagBFP2 (BFP) as the intermediate fluorophore. The experiment was carried out as in Fig. 2*E*. (*C*) Spectral profile of a SRET^2 experiment carried out as in Fig. 2 *A*–*C* using SRET^2 settings. (*D*) Titration curves in the BRETFect setup with increasing concentrations of the acceptor (CoA-Ven); the *x* axis represents measured acceptor (Venus) fluorescence over combined total output potential (CTOP). (*E*) Stimulated fluorescence readings and recorded luminescence of cells of the titration assays in *D* with associated BRET(550/485) ratios. (*F*) Titration curves in the BRETFect setup with increasing concentrations of the intermediate (ERα-mTFP1); the *x* axis represents measured intermediate fluorescence (mTFP1) over CTOP. Titrations with unfused ER were performed by adding the same amounts of the corresponding expression vector. (*G*) Stimulated fluorescence readings and recorded luminescence of cells of the titration assays in *F* with associated BRET(550/485) ratios. (*H*) Experiments were carried out as in Fig. 2*E* using control noninteracting proteins for the acceptor (mCoA-Ven) or intermediate (Nur77-mTFP1, ERα (L507R)-mTFP1), or no intermediate. All graphs were prepared from at least three biological replicates, and error bars represent the SEM.

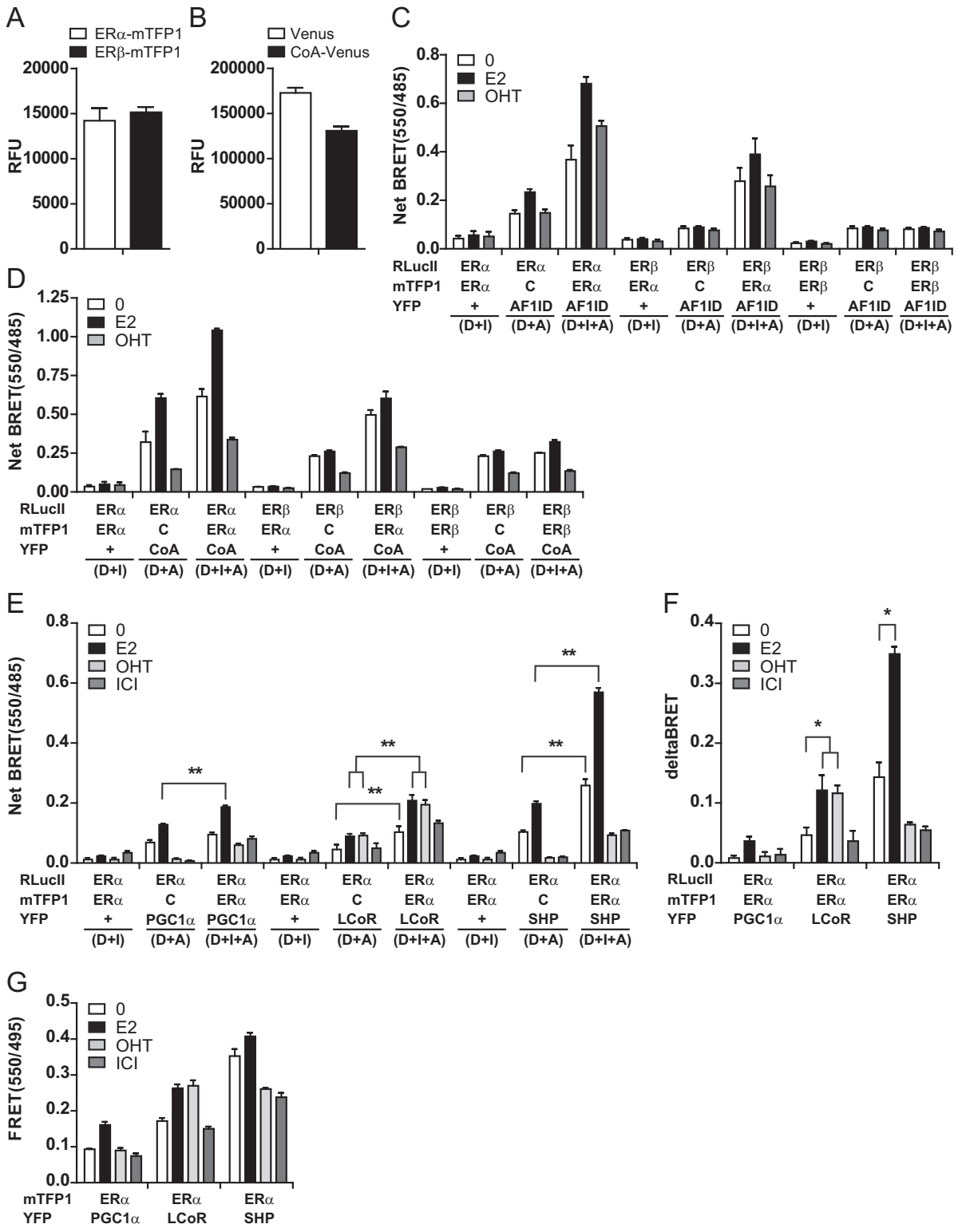

Fig. S3. (*A*) mTFP1-tagged ERα and ERβ fusion proteins used in Figs. 3–5 are expressed at similar levels as revealed by fluorometry. RFU, relative fluorescence unit. (*B*) Expression of Venus-tagged acceptor fusion proteins used in Fig. 3 *A* and *B* monitored by fluorometry. (*C*) BRETFect assays for AF1ID recruitment by ER dimers were reproduced in U2OS cells. Cells were treated as in Fig. 3*C*. (*D*) BRETFect assays for CoA recruitment by ER dimers were reproduced in U2OS cells. Cells were treated as in Fig. 3*A*. (*E*) BRETFect analysis of ligand-dependent recruitment of the cofactors PGC1α, LCoR, and SHP to ERα dimers. HEK293T cells were transfected with expression vectors for ERα-RLucII, ERα-mTFP1, and/or cofactors fused to Topaz and treated with the indicated ligands (1 μM) for 45 min. (*F*) Delta BRET calculations were performed from BRETFect assays in *E*. (*G*) FRET between the intermediate and acceptor in the BRETFect assays in *E*. HEK293T cells were transfected with ERα-mTFP1 plus the indicated constructs and treated with the indicated ligands (E2, OHT, or ICI) or with vehicle only (0) for 45 min. All graphs were prepared from at least three biological replicates, and error bars represent the SEM. Statistical significance was analyzed by ANOVA with a Bonferroni post hoc test. $*P < 0.01$, $**P < 0.001$.

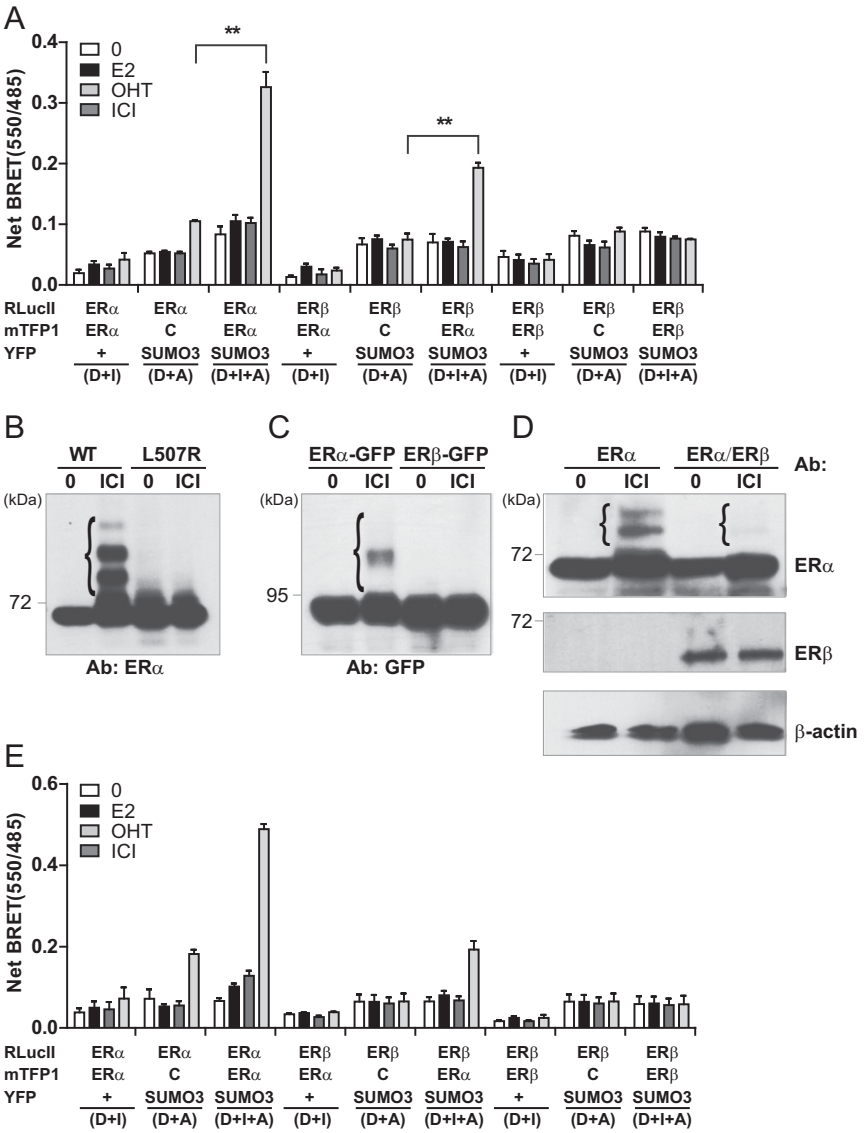

Fig. S4. (*A*) BRETFect assays for SUMOylation of ER dimers. Cells were transfected with expression vectors for ERα-RLucII, ERβ-mTFP1, and/or SUMO3 fused to eYFP and treated for 2 h with 1 μM E2, OHT, or ICI182,780. Net BRET signals are shown. (*B*) Dimerization is required for SUMOylation. HEK293T cells were transfected with vectors expressing ERα (WT) or the dimerization-deficient mutant L507R and treated for 3 h with ICI182,780 or vehicle only (0). Western analysis was carried out with an antibody against ERα. (*C*) ERβ is not SUMOylated in response to ICI. HEK293T cells were transfected with vectors expressing ERα-GFP or ERβ-GFP and treated as in *B*. Western analysis was carried out with an antibody against GFP. (*D*) ERα–ERβ heterodimers show weaker SUMOylation marks. HEK293T cells were transfected with vectors expressing ERα (WT) either alone or in combination with ERβ (WT) and treated for 3 h with ICI182,780 or vehicle only (0). Western analysis was carried out with antibodies against ERα, ERβ, or β-actin. (*E*) BRETFect assays for SUMOylation of ER dimers were reproduced in U2OS cells. Cells were treated as in *A*. Error bars represent the SEM. Statistical significance was analyzed by ANOVA with a Bonferroni post hoc test. $^{**}P < 0.001$.

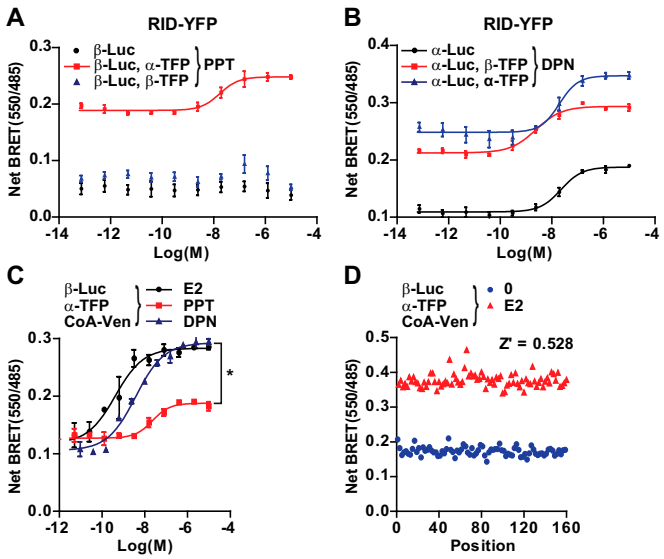

Fig. S5. (*A* and *B*) PPT (*A*) and DPN (*B*) promote the recruitment of the SRC1 RID to heterodimers. Experiments were carried out as in Fig. 5 *C* and *D* with the substitution of CoA-Venus for the SRC1 RID fused to Topaz (RID-YFP). (*C*) Net BRET ratios from cells transfected with ERα-RucII, ERα-mTFP1, and CoA-Venus and treated with varying concentrations of E2, PPT, or DPN. *$P < 0.01$ (Student's *t* test). (*D*) Z' score calculated from cells transfected with ERβ-RLucII, ERα-mTFP1, and CoA-Ven, seeded in two 96-well plates, and treated in alternate rows with estradiol (E2; 1 μM) or vehicle only (0). BRET ratios from individual wells are plotted on the graph against the position of the wells. All graphs were prepared from three biological replicates, and error bars represent the SEM.

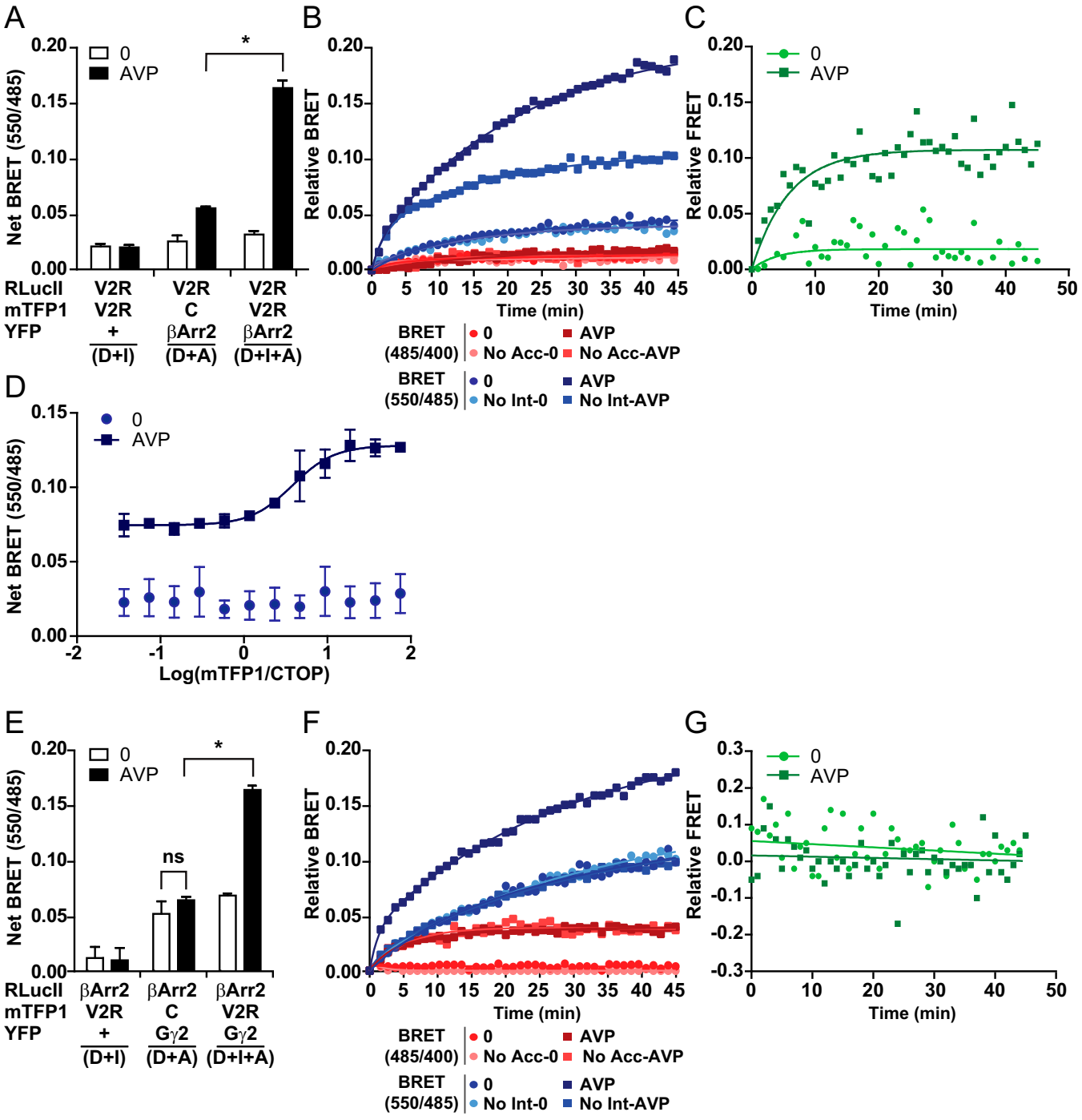

Fig. S6. (*A*) BRETFect assays for the recruitment of beta-arrestin2 to V2R dimers. Net BRET(550/485) signals were measured in the binary and ternary conditions in HEK293T cells expressing V2R fused to RLucII (donor), βArr2 fused to Venus (acceptor), or Venus alone, and mTFP1-tagged V2R as intermediate or untagged V2R (control C), after treatment with AVP (1 μM) or vehicle (0) for 20 min. Delta BRET signals are shown in Fig. 6*A*. (*B* and *C*) BRET (*B*) and FRET (*C*) signal increases recorded in the time course experiment from Fig. 6*B* and used to calculate delta BRET/FRET values in the presence vs. absence of AVP. (*D*) Titration curves showing BRETFect signal amplification dependence and saturation with increasing concentrations of the intermediate (V2R-mTFP1); *x* axis values are the log10 ratio of measured intermediate fluorescence (mTFP1) over CTOP. (*E*) BRETFect assays for the corecruitment of βArr2 and Gγ2 to V2R. Net BRET(550/485) signals were measured in HEK293T cells expressing βArr2 fused to RLucII (donor), Gγ2 fused to Venus (acceptor) or Venus alone, and mTFP1-tagged V2R (intermediate) or untagged V2R (control C), after treatment with AVP (1 μM) or vehicle (0) for 20 min. Delta BRET signals are shown in Fig. 6*C*. (*F* and *G*) BRET (*F*) and FRET (*G*) signal increases recorded in the time course experiment from Fig. 6*D* and used to calculate delta BRET/FRET values in the presence vs. absence of AVP. Error bars represent the SEM. Statistical significance was analyzed by ANOVA with a Bonferroni post hoc test. *$P < 0.01$.

Table S1. Allosteric effects between dimeric partners for recruitment of the coactivator motif peptide revealed by BRETFect titration curves with receptor-selective ligands

	EC_{50}, nM (95% confidence interval)		
Ligand	ERα–ERα	ERα–ERβ	ERβ–ERβ
E2	0.341 (0.255 to 0.481)	0.419 (0.214 to 0.822)	0.469 (0.222 to 0.831)
PPT	0.547 (0.421 to 2.22)	28.4 (10.3 to 38.6)	n/a
DPN	20.1 (15.2 to 40.4)	5.11 (2.76 to 11.8)	1.02 (0.196 to 2.12)

EC_{50}s are taken from curves in Fig. 5. Note that titration curves using inverted tagging of LucII and mTFP1 for the heterodimers yielded similar results. Data are the average of three biological replicates. n/a, not applicable.

Table S2. Allosteric effects between dimeric partners for recruitment of SRC1 RID revealed by BRETFect titration curves with receptor-selective ligands

	EC_{50}, nM (95% confidence interval)		
Ligand	ERα–ERα	ERα–ERβ	ERβ–ERβ
E2	0.404 (0.268 to 0.784)	0.503 (0.109 to 2.65)	0.218 (0.166 to 0.286)
PPT	0.968 (0.729 to 1.18)	25.1 (7.43 to 84.7)	n/a
DPN	69.7 (35.1 to 447)	17.6 (4.12 to 22.3)	0.757 (0.318 to 1.80)

EC_{50}s are taken from curves in Fig. S5 *A* and *B*. Note that titration curves using inverted tagging of LucII and mTFP1 for the heterodimers yielded similar results. Data are the average of three biological replicates. n/a, not applicable.